Anodic Aluminum Oxide Templated Channel Electrodes via Atomic Layer Deposition

A. B. F. Martinson[a,b], J. W. Elam[b], J. T. Hupp[*,a], M. J. Pellin[b]

[a] Department of Chemistry, Northwestern University, Evanston, Illinois 60208, USA
[b] Argonne National Lab, Division of Materials Science, Argonne, Illinois 60439, USA

Dye-sensitized solar cells (DSSCs) utilize high surface area metal oxide sintered particle networks to absorb molecular dyes and transport injected charge carriers. While this sintered particle architecture allows liquid electrolyte DSSCs to achieve efficiencies up to 11%, slow charge transport through the semiconductor network limits the amount of modification that can be made to the electrolyte and dye without adversely affecting the efficiency. The functionalization of anodic aluminum oxide membranes with thin films of transparent, semiconducting oxides via atomic layer deposition may allow for significantly faster charge transport. We demonstrate the fabrication of ZnO thin films within and upon commercially available anodic aluminum oxide membranes via atomic layer deposition.

Introduction

Dye sensitized solar cells (DSSCs) comprise an increasingly attractive alternative energy conversion technology.(1, 2) These photoelectrochemical cells use molecular dyes to sensitize high area, wide band gap semiconductor oxide photoanodes. Typically, a liquid electrolyte based on iodide/triiodide scavenges the hole left on the dye and shuttles it to a Pt-coated counter electrode where the circuit is completed. Solid-state (molecular or polymeric) hole scavenger/conductor have also been used.(2) The most efficient DSSCs convert AM1.5 solar insolation to electrical energy with 11% efficiency, but suffer from relatively poor photovoltages due to the overpotential needed to drive the dye regeneration reaction. Furthermore, they show less than optimal photocurrents due to insufficient light collection at wavelengths > 700 nm.(3)

Compared to the most efficient nanocrystalline TiO_2 photoanodes, devices fabricated with ZnO electrodes show significantly lower conversion efficiencies (4%).(4-6) Despite superior recombination dynamics, poor dye loading and charge injection into ZnO reduce the total photocurrent yield.(7) Yet ZnO DSSCs continue to be actively investigated due to the ease with which alternative and potentially superior high-area semiconductor morphologies may be fabricated. Particularly interesting are nominally 1-D arrays. Compared with standard photoanodes based on sintered nanocrystalline particles, 1-D photoanodes should show significantly faster electron transport, owing to a more direct path to the conductive glass electrode combined with fewer sites for trapping electrons. To this end, several novel photoanode architectures have been fabricated, including but not limited to hydrothermally grown ZnO nanorod arrays, electrodeposited ZnO platelets, and TiO_2 pores formed via titanium anodization.(8-10) In the most successful application of this idea to date, a 1.5% efficient ZnO nanorod array has been shown to exhibit significantly faster transport compared to nanoparticle networks.(11, 12) The efficiency

of the nanorod devices, however, is limited by the low surface area of the framework. Increasing the surface area of the nanorod array depends on growing higher aspect ratio rods via hydrothermal methods, which remains a significant challenge.(13)

Here we report a novel 1-D photoanode design with the potential for surface areas comparable to nanocrystalline sintered particle networks. Using anodic aluminum oxide (AAO) membranes as an inert and transparent template, atomic layer deposition (ALD) is utilized to grow thin films of transparent, semiconducting oxides on the pore wall. The result is a metal oxide general route to arrays of nanotubes suitable for use in DSSCs.

Experimental

For the ZnO-based cells, a 64 μm thick membrane with 210 nm pores that is 25-50% porous (Anodisc, Whatman) was coated with ZnO by ALD via alternate exposure to diethyl zinc and water at 200°C. The membranes were then fired at 400ºC in air for 30 minutes. A 1 μm thick electrode composed of transparent, conductive aluminum-doped zinc oxide (AZO) was deposited on one side of the membrane side ALD. The commercial AAO membranes employed in this study have pores that narrow to 20 nm within the last micron of thickness of one side. During deposition of the thick electrode, a steel fixture masked all but the small-pore face of the membrane. To improve the electrical contact to the AZO coating, Au was evaporated onto the coating along the edges of the AAO membrane.

After heating to 200ºC and subsequent cooling to 80ºC the warm membranes were soaked in 0.5 mM $(Bu_4N)_2[Ru(4,4'\text{-}(COOH)\text{-}2,2'\text{-}bipyridine)_2(NCS)_2]$ ("N719", Dyesol, B2 dye) in ethanol for 30 min followed by a quick rinse with acetonitrile. A 50 μm thick Surlyn frame separated the open-pore side of the membrane and a platinized fluorine-doped tin oxide (FTO) electrode. Light pressure was applied at 130ºC to seal the cell. A solution of 0.5 M LiI, 0.05 mM I_2, and 0.5 M *t*-butylpyridine in 3-methoxypropionitrile was introduced into the cell via vacuum backfilling through a hole in the FTO electrode. Additional Surlyn and a microscope cover slip sealed the electrolyte into the cell. Active areas were limited to 0.28 cm^2. AM1.5 efficiencies were measured on a Class A solar cell analyzer from Spectra-Nova Technologies.

Results and Discussion

As expected for an ALD sequence entailing sufficient exposure times, the resulting polycrystalline ZnO film is continuous and conformal, Figure 1. Measurements of the resistance through the 64 μm thickness of the membrane (~48 Ω, 8 nm thick ZnO) provide additional evidence that coatings span the length of the pores. As-deposited, ALD ZnO has numerous oxygen vacancies that make films moderately conductive and account for the relatively low resistance. A ZnO grain size of ~20 nm may be directly observed by SEM and is corroborated by X-ray diffraction data.

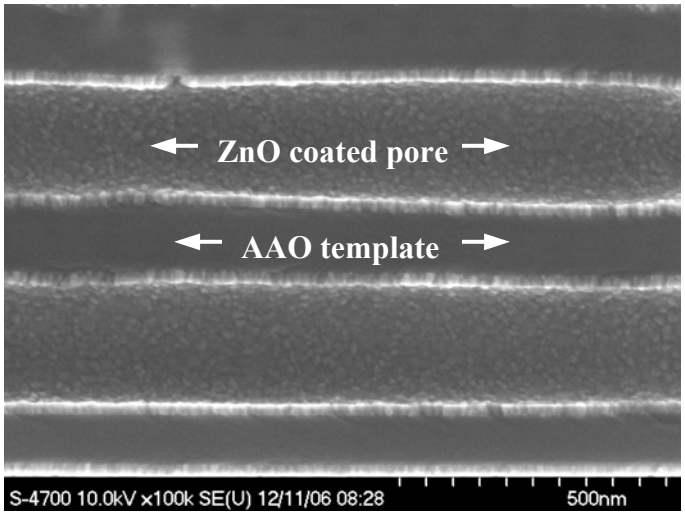

Figure 1. Commercial AAO template conformally coated with 20 nm of ZnO by ALD. Adapted from ref (14).

As shown in Figure 2, a thick coating of AZO was applied selectively to one side of the membrane by ALD. The combination of narrow pore termini and short exposure times (0.15 s) prevented the typically conformal deposition technique from significantly coating the pore interiors.

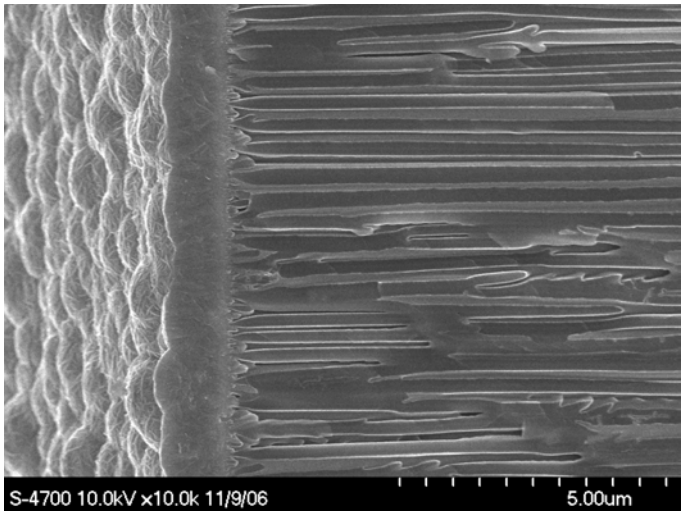

Figure 2. Commercial AAO template with thick AZO electrode deposited by ALD.

A large literature exists describing the theory and methodology for fabricating freestanding AAO membranes with hexagonally ordered pores ranging in size from 10-300 nm and pore densities in excess of 100 billion pores/cm^2.(15-17) For this study, commercial membranes with modest surface area were selected for their ready availability. The roughness factor of the commercial disc may be estimated from the geometry of hexagonally ordered pores:

$$RF = \frac{4\pi}{\sqrt{3}} \frac{rt}{s^2} \quad [1]$$

where r, t and s are the pore radius, membrane thickness, and center-to-center pore spacing, respectively. Although poorly ordered, an average spacing of 329 nm suggests an RF on the order of 450. The measured nitrogen isotherm on 50 discs yield a BET surface area of 9.02 m^2/g (Figure 3). The resulting roughness factor of approximately 485 agrees with the above calculations.

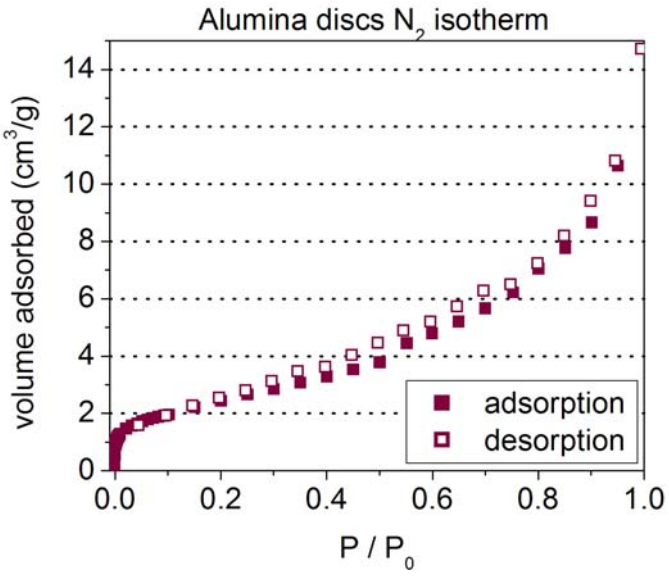

Figure 3. Nitrogen uptake of 50 commerical AAO membranes.

Figure 4 shows the AM1.5 power efficiency (η_p) for a series of devices with increasing nanotube wall thickness. In the control device, lacking ZnO, η_p is extremely low. This is not surprising given that the useful surface area is similar to that of a flat electrode. The facile parasitic reaction of the redox shuttle with the thick TCO electrode at the end of each pore may also limit performance. With the thinnest tube walls relatively small amounts of charge are collected by the AZO electrode, most likely due to a combination of slow charge transport through the ZnO and accelerated recombination owing to high steady-state concentrations of injected electrons. As the nanotube walls thicken, electrons flow more freely and η_p increases to a peak of value of 1.6%. Subsequent tapering with thicker walls is consistent with decreasing surface area, and therefore light harvesting efficiency, due to a smaller pore radius. (Figure 5).

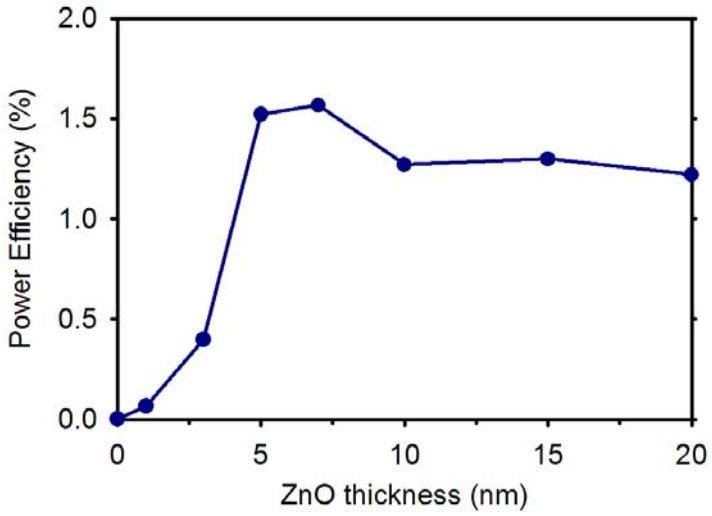

Figure 4. Power conversion efficiency under AM1.5 illumination as a function of ZnO nanotube wall thickness.

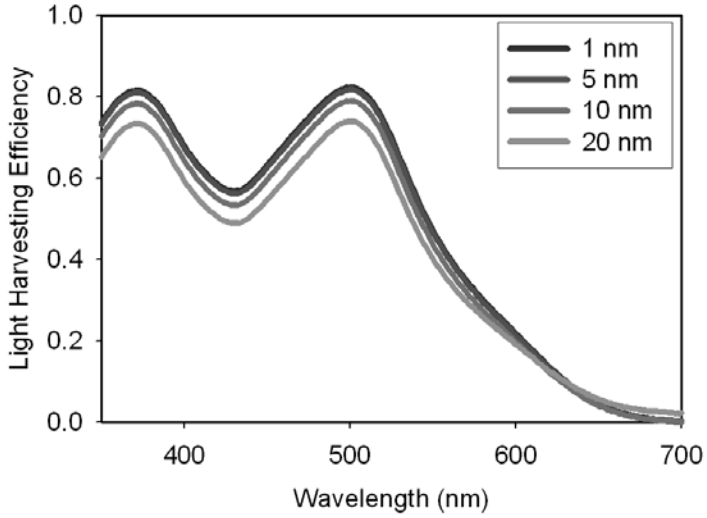

Figure 5. Light harvesting efficiency of dye desorbed from photoanodes with increasing ZnO pore wall thickness.

Conclusion

ZnO channel electrodes have been incorporated into dye-sensitized solar cells where they display reasonable light harvesting efficiency and moderate power efficiency. While the novel devices compare favorably with other ZnO-based DSSCs, an increased surface area will clearly be needed in order to obtain overall energy conversion efficiencies approaching that of the best ZnO cells. Current research is focused on determining the extent to which custom-made membranes and other semiconductors may improve photoanode performance.

Acknowledgments

The work at Northwestern is supported by the U.S. Department of Energy, Basic Energy Sciences Program, under Grant DE-FG02-87ER13808 and by BP Solar. Work at Argonne is supported by the U.S. Department of Energy, BES-Materials Sciences under Contract W-31-109-ENG-38. Electron microscopy was performed at the Electron Microscopy Center for Materials Research at Argonne National Laboratory, a U.S. Department of Energy Office of Science Laboratory operated under Contract No. DE-AC02-06CH11357 by UChicago Argonne, LLC. We thank Tobin Marks for use of the solar cell analyzer and Karen Mulfort for BET analysis.

References

1. Gratzel, M., *Inorg. Chem.* **44,** 6841 (2005).
2. Gratzel, M., *MRS Bull.* **30,** 23 (2005).
3. Nazeeruddin, M. K.; DeAngelis, F.; Fantacci, S.; Selloni, A.; Viscardi, G.; Liska, P.; Ito, S.; Takeru, B.; Gratzel, M., *J. Am. Chem. Soc.* **127,** 16835 (2005).
4. Kakiuchi, K.; Hosono, E.; Fujihara, S., *J. Photoch. Photobio. A* **179,** 81 (2006).
5. Hosono, E.; Fujihara, S.; Honma, I.; Zhou, H., *Advanced Materials* **17,** 2091 (2005).
6. Keis, K.; Magnusson, E.; Lindstrom, H.; Lindquist, S. E.; Hagfeldt, A., *Solar Energy Materials and Solar Cells* **73,** 51 (2002).
7. Quintana, M.; Edvinsson, T.; Hagfeldt, A.; Boschloo, G., *J. Phys. Chem. C* **111,** 1035 (2007).
8. Law, M.; Greene, L. E.; Johnson, J. C.; Saykally, R.; Yang, P. D., *Nat. Mater.* **4,** 455 (2005).
9. Yoshida, T.; Pauporté, T.; Lincot, D.; Oekermann, T.; Minoura, H., *J. Electrochem. Soc.* **150,** C608 (2003).
10. Paulose, M.; Shankar, K.; Varghese, O. K.; Mor, G. K.; Grimes, C. A., *J. Phys. D Appl. Phys.* **39,** 2498 (2006).
11. Martinson, A. B. F.; McGarrah, J. E.; Parpia, M. O. K.; Hupp, J. T., *Phys. Chem. Chem. Phys.* **8,** 4655 (2006).
12. Galoppini, E.; Rochford, J.; Chen, H.; Saraf, G.; Lu, Y.; Hagfeldt, A.; Boschloo, G., *J. Phys. Chem. B* **110,** 16159 (2006).
13. Greene, L. E.; Yuhas, B. D.; Law, M.; Zitoun, D.; Yang, P., *Inorg. Chem.* **45,** 7535 (2006).
14. Martinson, A. B. F.; Elam, J. W.; Hupp, J. T.; Pellin, M. J., *submitted* "ZnO Nanotube Based Dye-Sensitized Solar Cells" (2007).
15. Lee, W.; Ji, R.; Gösele, U.; Nielsch, K., *Nat. Mater.* **5,** 741 (2006).
16. Li, A. P.; Müller, F.; Birner, A.; Nielsch, K.; Gösele, U., *J. Appl. Phys.* **84,** 6023 (1998).
17. Masuda, H.; Yada, K.; Osaka, A., *Jpn. J. Appl. Phys.* **37,** L1340 (1998).